de Haas–van Alphen measurements on the antiferromagnet $URhIn_5$

Jing Fei Yu,[1,*] Attila Bartha,[2] Jeroen Custers,[2] and Stephen R. Julian[1,3]
[1]*Department of Physics, University of Toronto, Toronto, Ontario, Canada M5S 1A7*
[2]*Department of Condensed Matter Physics, Charles University, Ke Karlovu 5, 121 16 Praha 2, Czech Republic*
[3]*Canadian Institute for Advanced Research, 180 Dundas St. W, Toronto, Ontario, Canada M5S 1Z8*
(Received 29 May 2017; revised manuscript received 11 August 2017; published 21 September 2017)

We report on the results of a de Haas–van Alphen (dHvA) measurement performed on the recently discovered antiferromagnet $URhIn_5$ ($T_N = 98$ K), a $5f$ analog of the well studied heavy fermion antiferromagnet $CeRhIn_5$. We observe two small Fermi surfaces: a roughly spherical pocket β, with $F_\beta \simeq 0.3$ kT, and a pillow-shaped closed surface, α, with $F_\alpha \simeq 1.1$ kT. In addition, we observe two higher frequencies γ_1 with $F_{\gamma_1} \simeq 3.2$ kT and γ_2 with $F_{\gamma_2} \simeq 3.5$ kT that are seen only near the c axis, and that may arise on cylindrical Fermi surfaces. The measured cyclotron masses range from $1.9m_e$ to $4.3m_e$. A simple LDA+SO calculation performed for the paramagnetic ground state shows a very different Fermi surface topology, demonstrating a need for more advanced electronic structure calculations.

DOI: 10.1103/PhysRevB.96.115143

I. INTRODUCTION

Uranium-based compounds exhibit a wide range of exotic properties, from the unconventional superconductivity in heavy fermion UPt_3 [1] to the enigmatic hidden order in URu_2Si_2 [2], and all the way to weakly correlated metallic behavior in the uranium metal itself [2]. U atoms possess $5f$ electrons, whose spatial extent is greater than that of the $4f$ valence orbitals of the rare earths, but less than that of $3d$ orbitals of the row four transition metals [3]. Depending on their environment, the $5f$ electrons can be localized or itinerant (i.e., they may or may not be included in the Fermi volume) [4]. Moreover, uranium can have $5f$ valence ranging from $5f^3$ to $5f^0$, presenting further opportunities for inter- as well as intraorbital correlations and complexity.

For some uranium compounds such as the heavy fermion UPt_3 [1], the Fermi surface has been mapped and the $5f$ electrons are understood to be itinerant in character. On the other hand, the $5f$ electrons are fully localized in the related compound UPd_3 [5], while quantum oscillation data on the heavy fermion superconductor UPd_2Al_3 [6] has been explained by band-structure calculations in which some $5f$ electrons are localized on the U site, and others are itinerant band electrons [4]. Whether and when the $5f$ electrons are localized or itinerant, or partially localized, is still not well understood at present.

The focus of this paper is $URhIn_5$ (Fig. 1), a member of the U_nTX_{3n+2} ($n = 0,1,2$; T = transition metal; X = In, Ga) compounds. They are isostructural with the Ce_nTX_{3n+2} family [3]. In addition to the open question of the character of the $5f$ electrons, these compounds are also generally interesting because the system has a layered tetragonal structure, which means that adding layers of TX_2 can change the dimensionality from three dimensional to two dimensional [3].

$URhIn_5$ has been well characterized along with its bilayer cousin, U_2RhIn_8 [3,7]. It is tetragonal with $HoCoGa_5$-type structure ($P4/mmm$). It orders antiferromagnetically at a Néel temperature of $T_N = 98$ K [3]. The Sommerfeld coefficient is given as $\gamma = 60.7$ mJ mol^{-1} K^{-2} with Debye temperature $\Theta_D = 165$ K in Ref. [3], whereas $\gamma = 50$ mJ mol^{-1} K^{-2}, $\Theta_D = 187$ K are reported by Ref. [8]. The Sommerfeld coefficient is similar to that of $UNiGa_5$ [9], and rather large considering the high Néel temperature. The magnetic moment, $\mu_{\text{eff}} = 3.6\mu_B/U$ [3], is close to the U^{4+} ($5f^2$) moment of $3.58\mu_B/U$ [9]. These are again properties very similar to $UNiGa_5$ [9].

Zero-field NMR and nuclear quadrupole resonance measurements have been performed on $URhIn_5$ [10]. The nuclear relaxation rate $1/T_1T$ satisfies the Korringa relation just below $T^* \approx 150$ K, which has led to the suggestion that the $5f$ electrons are localized above T^* and itinerant below [10]. The antiferromagnetic (AFM) propagation vector is commensurate, with propagation vector $\mathbf{Q} = (1/2,1/2,1/2)$ as determined unambiguously by a recent neutron diffraction study [11]. Interestingly, $UNiGa_5$ also exhibits the same ordering vector [10].

Matsumoto *et al.* [7] have previously reported dHvA quantum oscillations in $URhIn_5$. They only observed two frequencies along [100], 1.1 kT and 720 T, with angle dependence suggesting that they both arise on a small ellipsoidal pocket. The presence of a small pocket is consistent with the nonmagnetic, $5f$ itinerant semimetal $URhGa_5$ [12], but the authors note that the large specific heat found in the antiferromagnetic state of $URhIn_5$ cannot be explained by this pocket alone, suggesting the likely existence of larger Fermi surfaces undetected by their study. In comparison, quantum oscillation measurements on $UNiGa_5$ show two cylindrical surfaces (0.8 kT and 1.3kT) along with two larger ellipsoidal surfaces (2.6 and 1.6 kT), but additional heavier Fermi surfaces would again be needed to explain the large specific heat [9]. On the other hand, a larger Fermi surface (4 kT) has been detected, in addition to smaller pockets, in UIn_3, the $n = \infty$ member of the U_nTX_{3n+2} family, although additional, multiconnected surfaces are still needed for γ to match experimental values [13].

Recently, magnetoresistance and Hall resistance also have been measured on $URhIn_5$ [14]. The magnetoresistance follows the H^2 behavior at higher temperatures but deviates from it for temperatures below 30 K [14]. At low temperature the magnetoresistance is positive, but the angle dependence,

*jfeiyu@physics.utoronto.ca

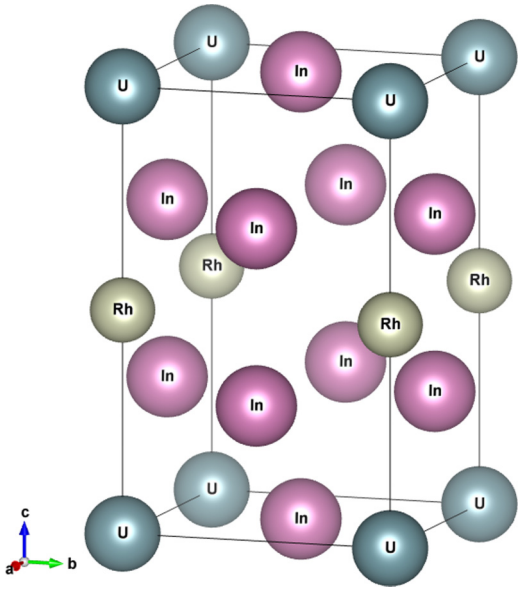

FIG. 1. Crystal structure of $URhIn_5$, visualized using VESTA software [15].

which could reveal the presence of open orbits, has not been reported. The Hall resistance R_H is negative below the Néel temperature (T_N), suggesting that the electronlike carriers dominate electronic transport [14].

Motivated by these previous measurements, we performed a quantum oscillation measurement on high-quality $URhIn_5$ samples. In this paper, we present these results in detail.

II. SAMPLES AND EXPERIMENTAL METHOD

Three high-quality crystals of $URhIn_5$, prepared using the self-flux method [3], were used. The samples were characterized by energy-dispersive x-ray analysis, Laue diffraction, and specific heat before the experiment was performed. Specific heat measurements revealed trace amounts of U_2RhIn_8 in two of the three samples, in the form of a broad peak at the $T_N = 117$ K of U_2RhIn_8, but in the third sample no impurity phases were seen. No peaks were seen at 88 K for any of the samples used, indicating that they were free from any UIn_3 impurities. The ratio of room temperature to 4 K resistivity exceeded 200 [3], which indicates that the samples were of high quality. Indeed, the observation of quantum oscillations, as described below, is itself an indicator of good sample quality, and one of the most appealing features of quantum oscillation measurements is that, when the sample quality is not uniform, the quantum oscillations arise predominantly from the cleanest parts of the crystal, so unlike most bulk measurements, quantum oscillations act like a filter for high-quality parts of the sample.

Modulation field de Haas–van Alphen measurements were carried out on these samples, with field ranges from 9 to 16 T and at temperatures between 65 and 2000 mK. The samples were rotated with respect to the applied field in the [001] to [100] plane and the [100] to [110] plane. Previous specific heat measurements [3] up to 9 T at low temperature showed no effect of magnetic field, and in our measurements, which track the susceptibility dM/dH, as well as the second-harmonic d^2M/dH^2, no anomalies were observed between 0 and 16 T, that might for example be associated with spin-flop transitions, so we believe that the magnetic field is not modifying the antiferromagnetism of the sample.

III. RESULTS

Figure 2(a) shows an example of our raw data from 10 to 16 T at 65 mK, with field tilted at 4° from [001], and Fig. 2(b) shows the Fourier transform of the same set of raw data. A very strong peak at 1.1 kT and its three harmonics can be easily seen. This frequency is labeled α. In addition, expending the vertical scale in Fig. 2(c), other sharp peaks are present as well: at 0.3, 3.2, and 3.5 kT. These are labeled β, γ_1, and γ_2, respectively.

The effective mass m^* associated with each extremal orbit can be extracted using the Lifshitz-Kosevich (LK) formula:

$$A = A_0 \frac{Cm^*T/B}{\sinh Cm^*T/B}, \tag{1}$$

where $C = \frac{2\pi^2 k_B m_e}{e\hbar}$, and A_0 is a constant. Typical fits are shown in Fig. 3. The cyclotron masses found for other directions are summarized in Table I.

The angle dependence of the dHvA frequencies is shown in Fig. 4. The β branch has very little angle dependence, which suggests that it arises from a nearly spherical Fermi surface. However, the lack of any significant angle dependence may also be a sign of an impurity phase from, say, the inclusion of flux used to grow the sample, or perhaps a spherical pocket in an impurity phase such as U_2RhIn_8. The α branch splits into two frequencies around 40°. This suggests a distorted sphere that has only one extremal orbit at the c axis, but two extremal orbits beyond a critical angle. The two branches γ_1 and γ_2 are close in frequency and it is natural to think that they arise on the same Fermi surface sheet: geometrically this would be certain only if they converge as the angle is rotated away from the c axis. But the frequency of γ_1 shows only a small upward curvature before it disappears. Thus we cannot rule out the possibility that they are distinct surfaces. γ_1 and γ_2 may arise from cylindrical surfaces, as shown from their upward curvatures. This is supported by the fact that we do not observe these frequencies at [100] or [110], which we would expect if this were a closed surface like α. However, as γ_1 and γ_2 disappear relatively quickly when we rotate away from the c axis, the evidence is not conclusive.

IV. ANALYSIS AND DISCUSSION

A. Paramagnetic ground-state calculation

We performed an LDA+SO calculation of $URhIn_5$'s ground state, using the linearized augmented plane wave (LAPW) scheme that was implemented in the WIEN2K package [16]. Spin-orbit coupling was turned on, and $RK_{\max}$ was set to 7.0. The resulting Fermi surface is shown in Fig. 5(a). Using the supercell K-space extremal area finder (SKEAF) [17] program, dHvA frequencies and approximate effective masses were extracted and are given in Table II. These values do not generally match the experimentally obtained values in Table I,

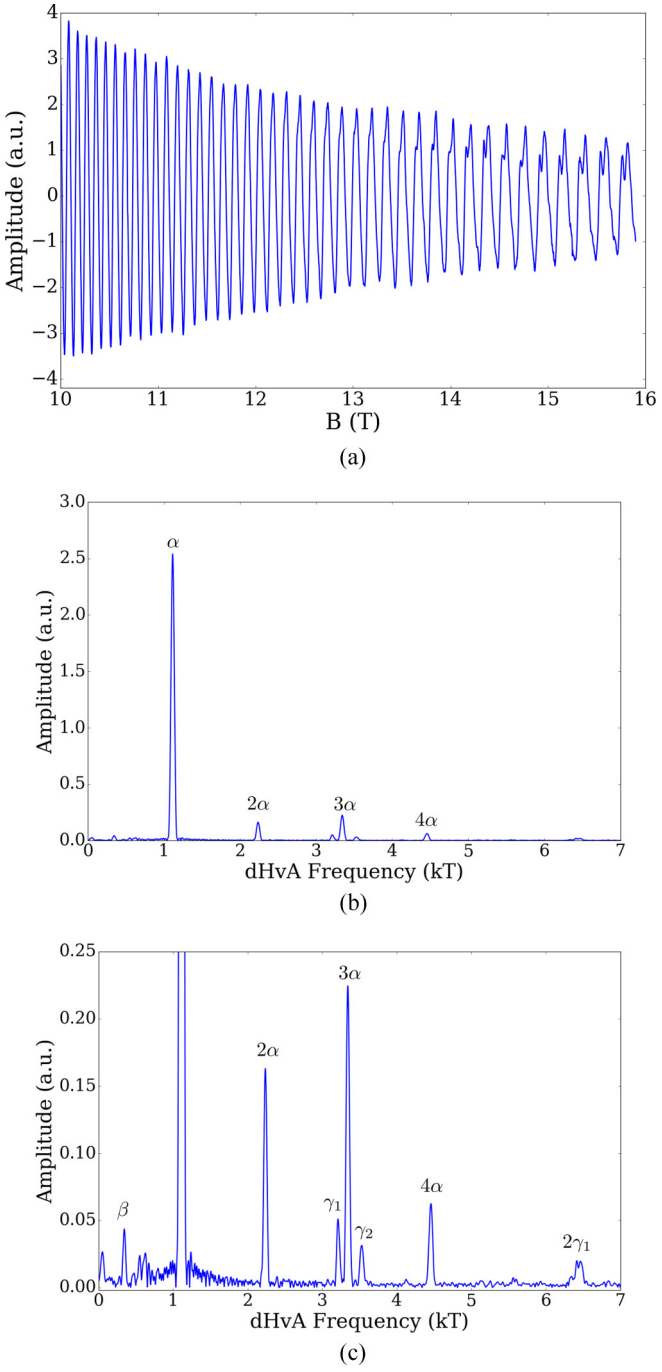

FIG. 2. (a) $URhIn_5$ quantum oscillations from 10 to 16 T, 65 mK. The field is 4° from [001]. (b) Fourier transform of the data in (a), showing a dominant α frequency that has been previously reported [7]. (c) The frequency spectrum of (b) with an expanded vertical scale, revealing several new frequencies, not observed in previous work [7].

however, band 48 does have a 1.1 kT frequency that is similar to our α branch.

To study this 1.1 kT frequency further, we used SKEAF to find the angle dependence of the frequencies, shown in Fig. 6. Here we can see that the 1.1 kT frequency is a closed ellipsoidal surface similar to our α branch. However, the difference from experiment is that a second, *higher* frequency of 1.5 kT branches out from the main frequency, whereas

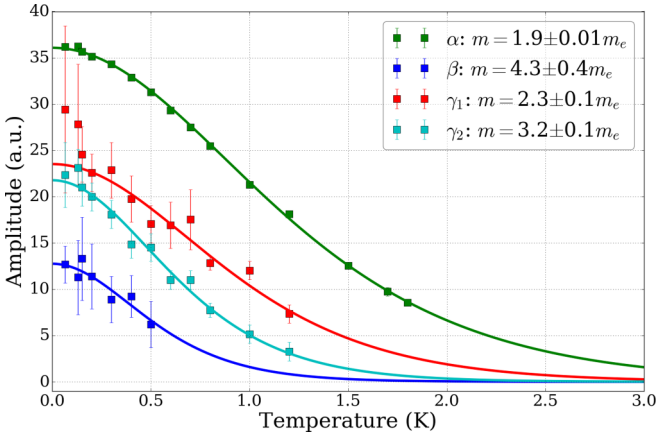

FIG. 3. Mass study of different dHvA frequencies with $B \parallel [001]$, using LK fit [Eq. (1)]. The error bars on the α branch are too small to be seen.

in the experimental results, a *lower* frequency branches out. The topology of the two Fermi surfaces is therefore not very similar. While the γ_1 and γ_2 frequencies in our experiment could be coming from cylindrical surfaces, they are almost ten times larger than the frequencies found by SKEAF in the paramagnetic WIEN2K calculation. Looking down along the c axis [Fig. 5(b)], one can see that several small surfaces contact the antiferromagnetic Brillouin zone (BZ) boundary. One can imagine that multiconnected surfaces across multiple BZs can be induced by the BZ folding resulting from the AFM ordering. This could be the origin of the large frequencies γ_1 and γ_2. However, simple band folding of the paramagnetic bands does not explain our experimental results (see Supplemental Material [18] for details on the band-folding calculation).

B. Fermi volume estimation

The total BZ volume is 1.6×10^{30} m^{-3}. If antiferromagnetism doubles the unit cell, the AFM BZ shrinks to 7.8×10^{29} m^{-3}. If we assume all the Fermi surface sheets are spherical so the volume of each sheet is given by $V = 4/3\pi k_F^3$, then given the antiferromagnetic BZ, α occupies 3.2% of the BZ, β occupies 0.4%, γ_1 occupies 16%, and γ_2 occupies 19% of the Brillouin zone. If we assume γ_1 and γ_2 are cylindrical surfaces and their volumes are given by $S_F \times 2\pi/c$ where S_F is the area enclosed by the cylinder and given by the dHvA frequency, c is the c-axis lattice parameter, and $2\pi/c$ is the

TABLE I. Summary of the experimental dHvA frequencies and fitted cyclotron masses m^*. Missing entries mean that the oscillation was only observed with the applied field along the c axis.

	$B \parallel [100]$		$B \parallel [110]$		$B \parallel [001]$	
Orbit	F (kT)	m^* (m_e)	F (kT)	m^* (m_e)	F (kT)	m^* (m_e)
β					0.3	4.3 ± 0.4
α	1.1	1.5 ± 0.02	1.1	2.0 ± 0.2	1.1	1.9 ± 0.01
γ_1					3.2	2.3 ± 0.1
γ_2					3.5	3.2 ± 0.1

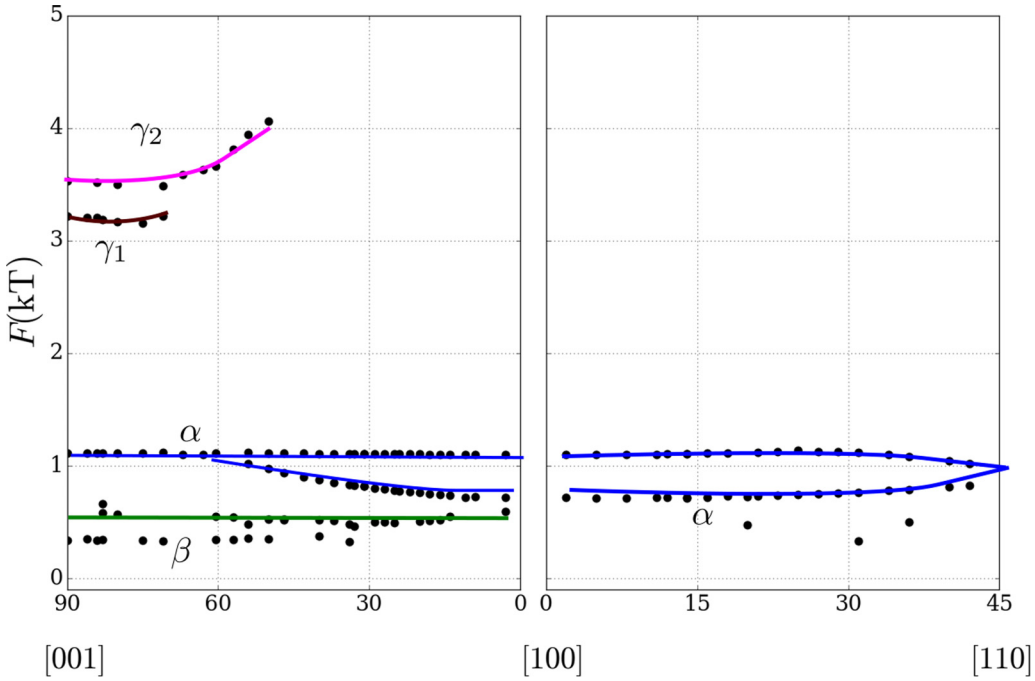

FIG. 4. dHvA frequency F vs θ, where θ is the angle between the magnetic field and the labeled crystalline axes. The data from [001] to [110] plane has been omitted as it is identical to that of [001] to [100]. The colored lines are guides to the eye.

height of the AFM BZ, the volumes of γ_1 and γ_2 become 33% and 36% of the total BZ volume, respectively. In total these Fermi surface sheets occupy nearly 73% of the total AFM BZ, if we assume there is only one copy of each Fermi surface in the BZ. As noted in the next section, however, it is probable that there are multiple copies of at least some Fermi surfaces.

C. Sommerfeld coefficient estimation

We can estimate the Sommerfeld coefficient $C/T = \gamma$ from the Fermi surfaces obtained. If we make the simplifying assumption that the frequencies at [001] correspond to spherical Fermi surfaces, so that the extremal area is given by $S_F = \pi k_F^2$, then α would contribute 1.7 mJ mol^{-1} K^{-2}, β would contribute 2.1 mJ mol^{-1} K^{-2}, γ_1 would contribute 3.6 mJ mol^{-1} K^{-2}, and γ_2 would contribute 5.2 mJ mol^{-1} K^{-2}. This sums up to 12.6 mJ mol^{-1} K^{-2} if we assume one sheet each, whereas the experimental value is around 50–60 mJ mol^{-1} K^{-2} [3,8].

If, however, we assume that γ_1 and γ_2 are distinct, cylindrical, Fermi surfaces, then their specific heat contributions are no longer k_F dependent and they rise to 4.9 mJ mol^{-1} K^{-2} for γ_1 and 6.8 mJ mol^{-1} K^{-2} for γ_2. The total C/T contribution then rises to 15 mJ mol^{-1} K^{-2} if we assume one copy of each sheet. This is still much too small. Thus we assume multiple copies of each sheet. For example, $4 \times \alpha$, $4 \times \beta$, $2 \times \gamma_1$, and $2 \times \gamma_2$ gives 38 mJ mol^{-1} K^{-2}, close to the range of the observed Sommerfeld coefficient, and the total BZ occupation will be around 87%. If, as seems more likely, γ_1 and γ_2 are extremal orbits on the same cylindrical Fermi surface, then

TABLE II. dHvA frequencies found using SKEAF, for $B \parallel [100]$, $B \parallel [110]$, and $B \parallel [001]$.

	B direction	F (kT)	m^* (m_e)
Band 47	[100]	1.1034	0.73
		1.1516	0.96
	[110]	0.1309	0.83
	[001]	0.2110	0.47
		0.2117	1.02
		0.3034	0.44
		0.5469	0.65
Band 48	[100]	1.0037	1.37
		1.5812	1.42
	[110]	1.1677	1.45
	[001]	1.0745	2.16

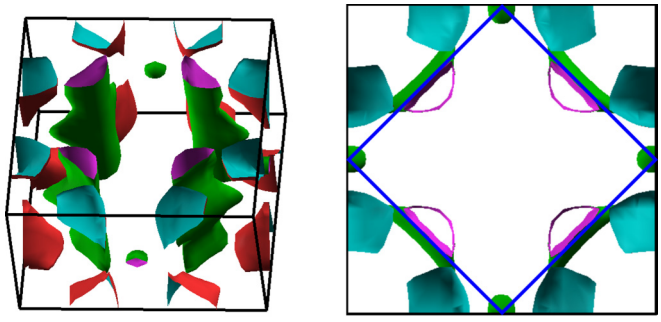

FIG. 5. (a) Fermi surface of the paramagnetic state in a single BZ, calculated by LDA+SO methods using the WIEN2K package [16]. Green: band 47; red: band 48. (b) Paramagnetic Fermi surface looking down from the c axis. Blue solid lines denote the antiferromagnetic BZ boundary.

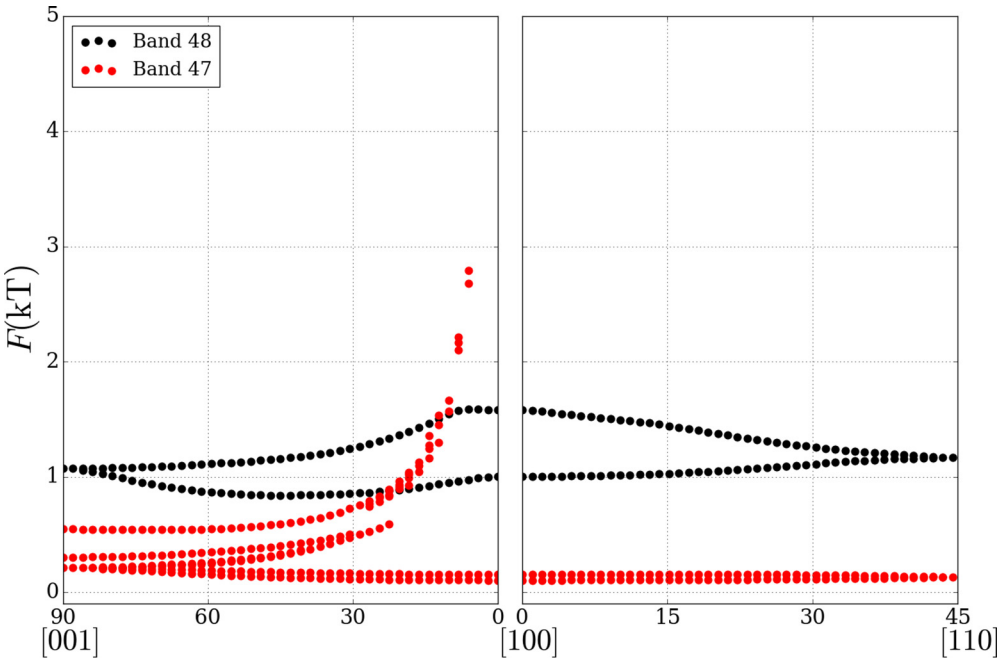

FIG. 6. dHvA frequency F vs θ found by SKEAF for the paramagnetic all-itinerant Fermi surface, where θ is the angle between the magnetic field and the labeled crystalline axes. For the corresponding surfaces to each band see Fig. 5(a) and its caption.

we can have $4 \times \gamma$ instead of $2 \times \gamma_1$, and $2 \times \gamma_2$ with an average contribution of 5.9 mJ mol^{-1} K^{-2} per sheet gives the same result. This scenario would account for all of the specific heat, but the BZ would be very packed. The only other possibility is that there are heavy orbits (i.e., hot spots) on the Fermi surface sheets that we have observed, or else other heavy surfaces that we have not observed. A better estimate of γ will be obtained once we have reliable band-structure calculations.

D. Comparisons to previous studies and other related compounds

Comparing our results to the earlier dHvA study on $URhIn_5$ by Matsumoto *et al.* [7], the frequency α and its splitting at higher angles were seen in both experiments. The angle dependence, which is indicative of an ellipsoidal Fermi surface, agrees well. In our experiment, however, we also observed two larger Fermi surface sheets, γ_1 and γ_2, as well as one additional small spherical pocket β. While the total contribution from the observed sheets to specific heat remains well under the experimental value of $\gamma = 50$–60 mJ mol^{-1} K^{-2}, we can at least consider the possibility of some combination of these sheets as mentioned in the section above, that will make up the missing specific heat contribution. The observation of these larger sheets also suggests that $URhIn_5$ is very different from the nonmagnetic, $5f$-itinerant semimetal $URhGa_5$ which has only small pockets and small specific heat [7,12].

In Ref. [7], a comparison was made to a reference compound $ThRhIn_5$, which has the same crystal structure but does not have $5f$ electrons. $ThRhIn_5$ has very large Fermi surfaces (up to 7 kT) and with strong angle dependence that would be expected for quasicylindrical surfaces [7,19]. These are considerably larger than our observations. However, as γ_1 and γ_2 are suggestive of being cylindrical surfaces, it may be that the electronic structure of $URhIn_5$ is not as drastically different from $ThRhIn_5$ as previously thought [7].

$UNiGa_5$ is another antiferromagnet in this family, with a Néel temperature $T_N = 85.5$ K and a Sommerfeld coefficient $\gamma = 30$ mJ mol^{-1} K^{-2} [9]. Its Fermi surface has also been mapped using dHvA. In $URhIn_5$, our α surface has a very different angular dependence from that of any of the ellipsoidal Fermi surfaces in $UNiGa_5$. The largest cylindrical Fermi surface in $UNiGa_5$, on the other hand, has a much smaller cross section for field along the c axis than our γ_1 and γ_2 surfaces. Whereas Tokiwa *et al.* see clear evidence of cylindrical Fermi surfaces [9], we were unable to follow our γ_1 and γ_2 frequencies far enough to confirm the $1/\cos\theta$ dependence expected for a cylindrical Fermi surface, but on balance it seems very likely that they arise on a cylindrical surface. The effective masses of $UNiGa_5$ at around 1.4–$3.1 m_e$ are, however, similar to those found for $URhIn_5$ [9]. While the paramagnetic state calculations do not match the experimental results for $UNiGa_5$ [9], advanced band-structure calculation for its antiferromagnetic ground state shows that the dHvA frequencies can be explained by $5f$ band magnetism [20].

As mentioned in the Introduction, another related compound to $URhIn_5$ is UIn_3. This compound is also an antiferromagnet and orders at $T_N = 88$ K [13]. It has a Sommerfeld coefficient of $\gamma = 40$ mJ mol^{-1} K^{-2}. The Fermi surface has been mapped, and no cylindrical Fermi surfaces were found [13]. The angle dependence does not resemble our findings for $URhIn_5$, and the effective masses of UIn_3 range from 9.8 to $33 m_e$, which are significantly larger than those of $URhIn_5$.

However, the lack of reliable band-structure calculations for $URhIn_5$ and UIn_3 [13] makes these comparisons quite speculative.

V. CONCLUSION

We remark that there are major discrepancies between the calculated $5f$ all-itinerant Fermi surface and the experimentally obtained dHvA frequencies, and the cyclotron masses also differ. The present results cannot be fully explained by the paramagnetic calculation and it is therefore highly desirable that a band-structure calculation be carried out for the antiferromagnetic ground state.

ACKNOWLEDGMENTS

J.C. would like to acknowledge many helpful discussions with M. Diviš. This work was generously supported by NSERC and CIFAR of Canada, Canada Research Chair, the Czech Science Foundation Grant No. P203/12/1201, and the Charles University project GAUK Grant No. 128317.

[1] G. J. McMullan, P. M. C. Rourke, M. R. Norman, A. D. Huxley, N. Doiron-Leyraud, J. Flouquet, G. G. Lonzarich, A. McCollam, and S. R. Julian, New J. Phys. **10**, 053029 (2008).
[2] J. A. Mydosh and P. M. Oppeneer, Philos. Mag. **94**, 3642 (2014).
[3] A. Bartha, M. Kratochvílová, M. Dušek, M. Diviš, J. Custers, and V. Sechovský, J. Magn. Magn. Mater. **381**, 310 (2015).
[4] G. Zwicknagl, A. Yaresko, and P. Fulde, Phys. Rev. B **68**, 052508 (2003).
[5] Y. Tokiwa, K. Sugiyama, T. Takeuchi, M. Nakashima, R. Settai, Y. Inada, Y. Haga, E. Yamamoto, K. Kindo, H. Harima, and Y. Onuki, J. Phys. Soc. Jpn. **70**, 1731 (2001).
[6] Y. Inada, H. Yamagami, Y. Haga, K. Sakurai, Y. Tokiwa, T. Honma, E. Yamamoto, Y. Ōnuki, and T. Yanagisawa, J. Phys. Soc. Jpn. **68**, 3643 (1999).
[7] Y. Matsumoto, Y. Haga, N. Tateiwa, E. Yamamoto, N. Kimura, H. Aoki, and Z. Fisk, in Proceedings of the International Conference on Strongly Correlated Electron Systems (SCES 2013) [J. Phys. Soc. Jpn. (2014)], Vol. 3, p. 011097.
[8] Y. Matsumoto, Y. Haga, N. Tateiwa, H. Sakai, T. D. Matsuda, E. Yamamoto, and Z. Fisk, Phys. Rev. B **88**, 045120 (2013).
[9] Y. Tokiwa, Y. Haga, E. Yamamoto, D. Aoki, N. Watanabe, R. Settai, T. Inoue, K. Kindo, H. Harima, and Y. Onuki, J. Phys. Soc. Jpn. **70**, 1744 (2001).
[10] H. Sakai, S. Kambe, Y. Tokunaga, Y. Matsumoto, N. Tateiwa, Y. Haga, and Z. Fisk, Phys. Rev. B **88**, 045123 (2013).
[11] A. Bartha, M. Klicpera, P. Čermák, B. Oluaddiaf, P. Javorský, and J. Custers (unpublished).
[12] S. Ikeda, Y. Tokiwa, T. Okubo, Y. Haga, E. Yamamoto, Y. Inada, R. Settai, and Y. Onuki, J. Nucl. Sci. Technol. **39**, 206 (2002).
[13] Y. Tokiwa, D. Aoki, Y. Haga, and E. Yamamoto, J. Phys. Soc. Jpn. **70**, 3326 (2001).
[14] Y. Haga, Y. Matsumoto, J. Pospíšil, N. Tateiwa, E. Yamamoto, T. Yamamura, and Z. Fisk, J. Phys.: Conf. Ser. **807**, 012015 (2017).
[15] K. Momma and F. Izumi, J. Appl. Crystallogr. **44**, 1272 (2011).
[16] P. Blaha, K. Schwarz, G. Madsen, D. Kyasnicka, and J. Luitz, *WIEN2k, An Augmented Plane Wave+Local Orbitals Program for Calculating Crystal Properties* (Karlheinz Schwartz, Universitat Wien, Austria, 2011).
[17] P. Rourke and S. Julian, Comput. Phys. Commun. **183**, 324 (2012).
[18] See Supplemental Material at http://link.aps.org/supplemental/10.1103/PhysRevB.96.115143 for results of an AFM band-folding calculation based on the all-itinerant paramagnetic ground-state calculation presented in the main text.
[19] T. D. Matsuda, Y. Haga, E. Yamamoto, S. Ikeda, H. Shishido, R. Settai, H. Harima, and Y. Onuki, J. Phys. Soc. Jpn. **76**, 064712 (2007).
[20] H. Yamagami, Physica B **312-313**, 297 (2002).